The Nanocomposites of Zinc Oxide/L-Amino Acid-Based Chiral Poly(ester-imide) via an Ultrasonic Route: Synthesis, Characterization, and Thermal Properties

Shadpour Mallakpour,[1,2] Fatemeh Zeraatpisheh[1]

[1]*Organic Polymer Chemistry Research Laboratory, Department of Chemistry, Isfahan University of Technology, Isfahan 84156-83111, Islamic Republic of Iran*
[2]*Nanotechnology and Advanced Materials Institute, Isfahan University of Technology, Isfahan 84156-83111, Islamic Republic of Iran*

Received 26 January 2011; accepted 16 December 2011
DOI 10.1002/app.36686
Published online in Wiley Online Library (wileyonlinelibrary.com).

ABSTRACT: In this investigation, a chiral poly) ester-imide) (PEI) via direct polyesterification of *N,N′*-(pyromellitoyl)-bis-(L-tyrosine dimethyl ester) and *N*-trimellitylimido-L-methionine was prepared using the tosyl chloride/pyridine/*N,N′*-dimethylformamide system as a condensing agent. This approach allows the insertion of two natural amino acids into the polymer backbone and the creation of a bioactive polymer. From the chemical point of view, the ester groups impart to the polymer's main and side chain increased sensibility to hydrolysis that can cause chain breaking. Therefore, this polymer is expected to be biodegradable and could be classified as an eco-friendly polymer. The polymer also had a useful level of thermal stability associated with excellent solubility. PEI/zinc oxide bionanocomposites were subsequently prepared by an ultrasonic method as a simple and inexpensive route, using ZnO nanoparticles (ZnO-NPs) modified by 3-aminopropyltriethoxylsilane (KH550) as a coupling agent. The structure and properties of the obtained BNC polymers were confirmed by Fourier transform infrared spectroscopy, X-ray diffraction, field emission scanning electron microscopy (FE-SEM), transmission electron microscopy (TEM), and thermogravimetric analysis (TGA). The direct proofs for the formation of the true BNC polymers were provided by TEM. Also, the morphology study of the synthesized polymer-based BNCs showed well-dispersed ZnO-NPs in the polymer matrix by FE-SEM analysis. TGA studies indicated that an increase of the NP content led to an enhancement of the thermal stability of the new BNC polymers. © 2012 Wiley Periodicals, Inc. J Appl Polym Sci 000: 000–000, 2012

Key words: ZnO nanoparticles; bionanocomposite polymers; thermally stable poly)ester-imide); ultrasonic irradiation; 3-aminopropyltriethoxylsilane (KH550)

INTRODUCTION

Nanotechnology has been defined as engineering and manufacturing at nanometer scales with atomic precision. Nanotechnology and bionanotechnology are exclusively novel concepts, invented late in the 20th century, and biotechnology has only been around for a few decades, and hence the scope of these fields is still being defined.[1] One of the most promising responses to decrease the human impact on the environment is the designing of bionanocomposites (BNCs) which consist of a biopolymer matrix reinforced with nanoparticles (NPs) having at least one dimension in the nanometer range (1–100 nm).[2] Polymer-based nanocomposite materials have been attracting immense interest from researchers as the mixing of nanoscale inorganic fillers into organic polymers, which possess interesting thermal,[3–5] electrical,[6] optical,[7] magnetic,[8] and mechanical[9] properties usually superior to those of the parent polymer or inorganic species. Therefore, these materials offer many potential uses in various areas such as biotechnology,[10] optics,[11] electronic devices,[12] and photocatalysis.[13] The most essential challenge in the preparation of these nanocomposite materials is to achieve a uniform distribution of the inorganic materials such as NPs in the polymer matrix. Regardless of the nature of filler material, nanoscale particles tend to agglomerate in organic matrix because of high-specific surface area and surface energy.[14] Some technical routes, such as encapsulating polymerization,[15] solution intercalation,[16] latex precompounding,[17] ultrasonic irradiation,[18] and the utilization of different coupling agents,[19] were developed for the improvement of the dispersion state of NPs in polymer matrix.

Correspondence to: S. Mallakpour (mallak@cc.iut.ac.ir or mallak777@yahoo.com or mallakpour84@alumni.ufl.edu).

Contract grant sponsors: Iran nanotechnology Initiative Council (INIC), National Elite Foundation (NEF), Center of Excellency in Sensors, Green Chemistry Research (IUT).

Among many inorganic NPs, nanosized zinc oxide (ZnO) is one of the most encouraging multifunctional materials in research. ZnO nanoparticles (ZnO-NPs) have numerous noteworthy chemical and physical properties, such as chemical stability, high luminous transmittance, high catalysis activity, effective antibacterial and bactericide function, intensive ultraviolet, infrared adsorption,[20–24] biocompatibility, high isoelectric point (9.5), fast electron transfer kinetics,[25] and nontoxicity.[26] The introduction of ZnO-NPs into polymer could improve the mechanical and optical properties of the polymer owing to their high-specific surface area, small size, quantum effect, and a strong interfacial interaction between the inorganic NPs and the organic polymer. Therefore, these nanocomposites could be widely applied in fibers, coatings, plastics, rubbers, sealants, and other applications.[27]

Poly(ester-imide) (PEI), as a type of macromolecules, is the combination of polyimide and polyester which could have properties of both of them and provide good balance between thermal stability and processability. In point of fact, PEIs are gaining wide acceptance by varied industries because they comprise a number of exceptional properties, such as good heat resistance, mechanical strength, electrical insulation, and other physical properties which are growing steadily.[28–30] Among them, chiral ones are significant polymers owing to their applications to catalysts, chromatographic supports, and materials with ferroelectric and nonlinear optical properties. The optical activity of the polymer can be tuned by choosing a suitable chiral initiator or by starting from a chiral monomer.[31,32]

Amino acid-derived functional polymers have been amassing much attention because of their biodegradability and biocompatibility, easing the environmental burden because amino acid residues can be targeted for cleaving by different enzymes. In continuation of our study for the preparation of thermally stable and optically active-modified polymers with amino acids, herein, we wish to report the synthesis and characterization of a PEI which has two different types of amino acid linkages in the main chain. Then, novel optically active PEI/zinc oxide bionanocomposites (PEI/ZnO BNCs) were synthesized through a simple and convenient ultrasonic wave dispersion process of modified nanostructure ZnO particles in the polymer matrix. The resulting BNC polymers are characterized by several techniques including Fourier transform infrared spectroscopy (FTIR), powder X-ray diffraction (XRD), thermogravimetric analysis (TGA), and their morphologies were investigated by field emission scanning electron microscopy (FE-SEM) and transmission electron microscopy (TEM) analysis.

EXPERIMENTAL

Materials

All chemicals were purchased from Fluka Chemical (Buchs, Switzerland), Aldrich Chemical (Milwaukee, WI), Riedel-deHaen AG (Seelze, Germany), and Merck Chemical *N,N′*-dimethylformamide (DMF) and pyridine (Py) were dried over barium oxide and then were distilled under reduced pressure. The silane coupling agent (3-aminopropyltriethoxylsilane) (KH550) was obtained from Merck Chemical. Nanosized ZnO powder was purchased from Neutrino (Tehran, Iran) with an average particle size of 25–30 nm. The amino acids were used as obtained without further purification.

Characterization

Infrared spectra of the samples were recorded at room temperature in the range of 4000–400 cm^{-1}, on (Jasco-680, Japan) spectrophotometer. The spectra of solids were obtained using KBr pellets. The vibrational transition frequencies are reported in wave numbers (cm^{-1}). Band intensities are assigned as weak (w), medium (m), strong (s), and broad (br). Proton nuclear magnetic resonance (^{1}H-NMR spectra, 500 MHz) was recorded in *N,N′*-dimethylsulfoxide (DMSO)-d_6 solution using a Bruker (Germany) Avance 500 instrument. Multiplicities of proton resonance were designated as singlet (s) and multiplet (m). Inherent viscosities were measured by a standard procedure using a Cannon-Fenske routine viscometer (Germany) at the concentration of 0.5 g/dL at 25°C. Specific rotations were measured by a Jasco Polarimeter (Japan). Thermogravimetric analysis (TGA) is performed with a STA503 win TA at a heating rate of 10°C/min from 25C to 800°C under nitrogen. The XRD pattern was acquired by using a Philips Xpert MPD X-ray diffractometer. The diffractograms were measured for 2θ, in the range of 10–80°, using Cu Kα incident beam (λ = 1.51418 Å). The dispersion morphology of the NPs on PEI matrix was observed using field emission scanning electron microscopy [FE-SEM, HITACHI (S-4160)]. Transmission electron microscopy (TEM) images were obtained using a Philips CM 120 microscope with an accelerating voltage of 100 kV.

Apparatus

The reaction was carried out by MISONIX ultrasonic liquid processors, XL-2000 SERIES. Ultrasonic irradiation was performed with the probe of the ultrasonic horn immersed directly in the mixture solution system with a frequency of 2.25×10^4 Hz and 100 W powers.

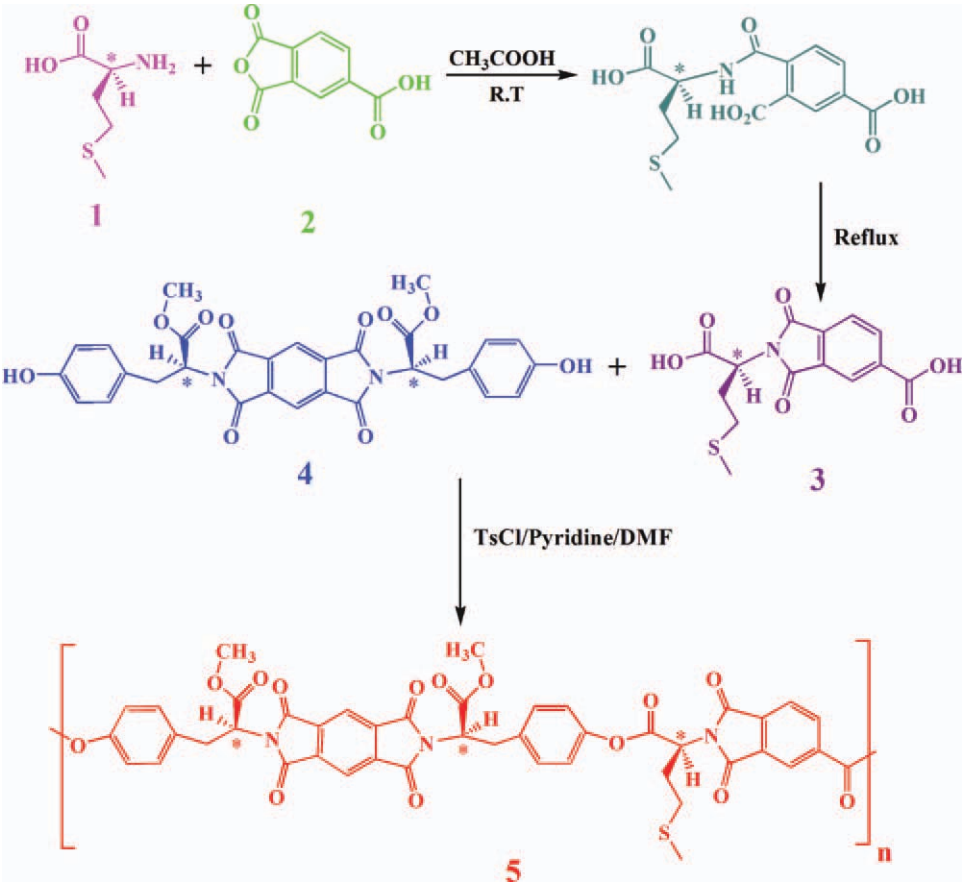

Scheme 1 Synthesis of the diacid and obtained PEI. [Color figure can be viewed in the online issue, which is available at wileyonlinelibrary.com.]

Polymer synthesis

N-trimellitylimido-L-methionine (3) as a diacid, *N,N′*-(pyromellitoyl)-bis-(L-tyrosine dimethyl ester) (4) as a diol, and PEI (5) (Scheme 1) were prepared according to our previous studies.[33–35]

Preparation of the PEI/ZnO BNCs

At first, ZnO-NPs were chemically functionalized with KH550 ($NH_2(CH_2)_3Si(OC_2H_5)_3$) using ultrasonic irradiation. For this purpose, ZnO-NP was dried at 110°C in an oven for 24 h to remove the adsorbed water. In total, 0.20 g of dried nano ZnO was ultrasonicated for 15 min in absolute ethanol, and then 0.08 g of KH550 was added to the system and ultrasonicated for 20 min. The mixture was filtrated and dried at 60°C for 24 h. The PEI/ZnO BNCs were synthesized via mixing the PEI with different amounts of modified ZnO-NPs (4, 8, and 12 wt %) in 20 mL of absolute ethanol followed by irradiation with high-intensity ultrasonic wave for 4 h. After irradiation, the solvent was removed and the obtained solid was dried in vacuum at 80°C for 2 h. The procedure for the preparation of PEI/ZnO BNCs is shown in Scheme 2.

RESULTS AND DISCUSSION

Synthesis and characterization of polymer

In this investigation, for the polycondensation of aromatic diacid and aromatic diol, a Vilsmeier adduct was prepared by dissolving TsCl in a mixed solvent of Py and DMF as condensing agent (Scheme 1). TsCl was dissolved in Py at room temperature and kept at this temperature for 30 min according to the previously reported methods that the appropriate aging time is 30 min.[36] It was concluded that a molar ratio of diacid over TsCl equals to 5 and the reaction time of 4 h is needed to generate a polymer with better yield and inherent viscosity. Furthermore, the reaction was run at 120°C as proposed by Higashi et al.[37] The inherent viscosity of the resulting polymer under optimized condition was 0.41 dL/g and the yield was 93%. The incorporation of chiral units into the polymer backbone was obtained by measuring the specific rotation of polymer which showed optical rotation and, therefore, is optically active {$[\alpha]^{25}_{Hg,365} = +160$ and $[\alpha]^{25}_{Na,598} = +18$ (0.05 g in 10 mL of DMF)}. This macromolecule showed good solubility in common dipolar organic solvent such as DMF, DMSO, *N,N′*-dimethylacetamide and *N*-

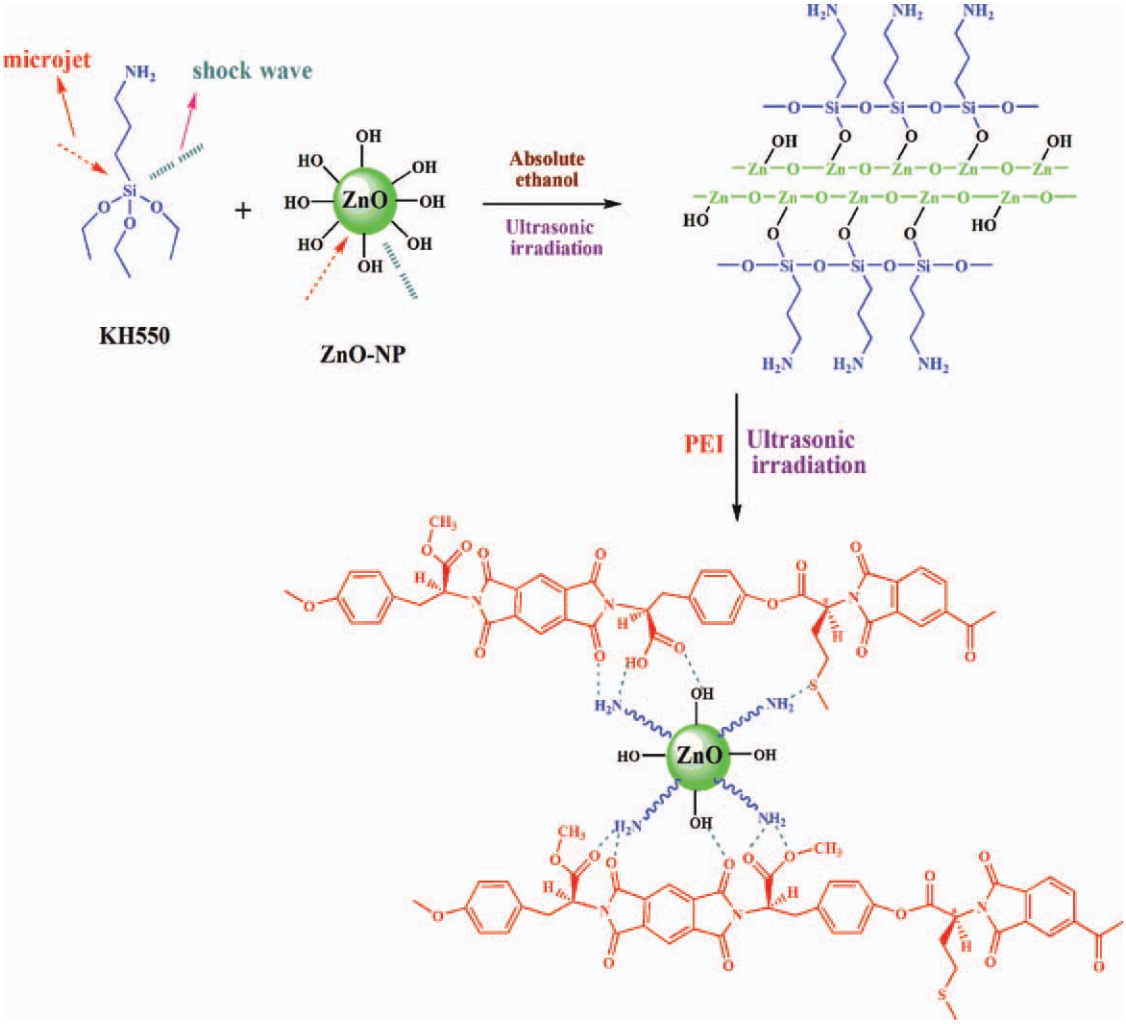

Scheme 2 Preparation of PEI/ZnO BNCs and illustration of the interaction between PEI and modified ZnO-NPs. [Color figure can be viewed in the online issue, which is available at wileyonlinelibrary.com.]

methyl-2-pyrrolidone. Other organic solvents such as acetone, cyclohexane, chloroform, methanol, and water did not solve the PEI. The resulting polymer was characterized by FTIR, ^{1}H-NMR spectroscopy techniques, and elemental analyses.[35] Polymers with chiral structures are biologically extremely prominent. Most of the natural polymers are optically active and have particular chemical activities such as catalytic properties that exist in proteins, genes, and enzymes. As a result, this polymer has potential to be used as chiral stationary phase in HPLC for the separation of racemic mixtures. Synthesis and characterization of optically active PEIs from diols and diacid chlorides under microwave irradiation was reported.[34,38,39] The direct polycondensation route avoids using moisture-sensitive acid chlorides and provides important benefits in manufacturing operations compared with conventional methods.

It is worth mentioning that to prepare biodegradable polymer 5, the diol 4 was employed whose biodegradability has been reported earlier by our group.[40] In addition, *in vitro* toxicity test was employed for evaluating the susceptibility of this polymer to microbial degradation. For this purpose, the monomer and prepared polymer were buried under the soil. The high microbial population and prominent dehydrogenase activity in the soil containing polymer confirmed that the synthesized polymer is biologically active and microbiologically biodegradable. Wheat seedling growth in the soil buried with synthetic polymer showed nontoxicity of polymer 5. For this cause, this multiblock copolymer with fine cytocompatibility is a desirable applicant as biodegradable and biologically active polymer.[41]

Preparation and FTIR characterization of PEI/ZnO BNCs

The interfacial interactions between the NPs and the polymer matrix play a crucial role in determining the quality and properties of the nanocomposite.[42]

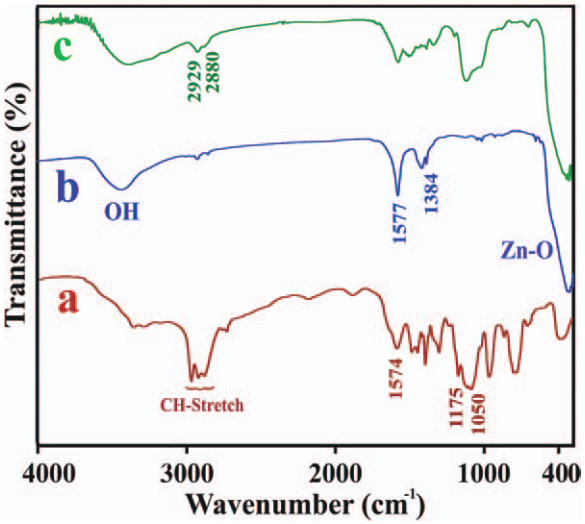

Figure 1 FTIR spectra of (a) KH550, (b) pure ZnO-NPs, and (c) ZnO-NPs modified by KH550. [Color figure can be viewed in the online issue, which is available at wileyonlinelibrary.com.]

However, ZnO-NP possesses large specific surface area and high surface energy, which may cause agglomeration of particles in polymer matrix and decline in performance of the nanocomposites. To improve the dispersion, ultrasonic irradiation and surface modification has been employed for producing nanostructural composites. The sonochemical reaction supplies appropriate reaction temperature to accelerate the hydrolysis of KH550. In addition, the microjets and shock waves created by intense ultrasonic waves in solution play a noteworthy role in the combination of hydrolyzed KH550 and ZnO sol. The collision chance of KH550 anchored onto the surface of ZnO sol particles is significantly increased.[43] Silanol groups of KH550 generated by hydrolysis can interact with hydroxyl groups on the ZnO-NPs surface and form the modification layer with —NH_2 groups. The functionalized NPs might be dispersed absolutely and will combine with PEI via the H-bonding of the unmodified —OH groups on the surface of ZnO-NPs and NH_2 of coupling agent with S and C=O groups in PEI. The details for fabrication mechanism of PEI/BNCs are shown in Scheme 2.

Figure 1 shows the infrared spectra of (a) KH550, (b) pure ZnO-NPs, and (c) KH550-modified-ZnO. In the spectrum of pristine ZnO-NPs, OH stretching band is observed at 3391 cm^{-1}. A strong band at 423 cm^{-1} is associated with the characteristic vibrational mode of Zn—O bonding.[44] Also, asymmetric and symmetric C=O stretching modes of zinc acetate are viewed at 1577 and 1384 cm^{-1}, respectively. The FTIR spectrum of the KH550-modified-ZnO [Fig. 1(c)] discloses some new peaks compared to pristine ZnO-NPs. As characteristic bands of KH550 molecules,[45] the stretching and bending modes of the —NH_2 group were viewed at 3355 and 1574 cm^{-1}, respectively. The absorption peaks at 1175 and 1050 cm^{-1} point to the presence of Si—O bonds which were attributed to the KH550 attachment.[46] In addition, the peak at 886 cm^{-1} can be assigned to the bending mode of Si—OH group.[45] As a result, the characteristic peaks of CH stretching band at 2880–2929 cm^{-1} in the infrared data of KH550-modified-ZnO-NPs compared to the infrared data of pure ZnO-NPs confirm that the connection is based on the covalent bonds between ZnO surface and KH550 molecules. FTIR spectrums of PEI and BNC polymers with different amounts of ZnO-NPs (4, 8, and 12 wt %) (Fig. 2) show the intensity of Zn—O stretching band raise with an increase of ZnO-NPs content in PEI.

X-ray diffraction data

The XRD patterns of (a) PEI, (b) ZnO-KH550, (c) PEI/ZnO BNC (4 wt %), and (d) PEI/ZnO BNC (12 wt %) are shown in Figure 3. It could be observed that there is a lack of any diffraction peak in the range of 2θ angle for PEI, and this X-ray diffractogram showed an amorphous diffraction pattern. The morphology of a polymeric material (i.e., amorphousness or semi-crystallinity) performs an important role in the degradation process. It is currently known that the crystallinity decreased the overall degradation rate of polymer in terms of weight loss.[47] Also, the crystallinity of polymers was usually reflected in their solubility behavior, which is in agreement with the general rule that the solubility decreases with increasing crystallinity.

The XRD patterns of BNCs indicate that the morphology of ZnO-NPs has not been changed during the process and the intensity of diffraction peaks

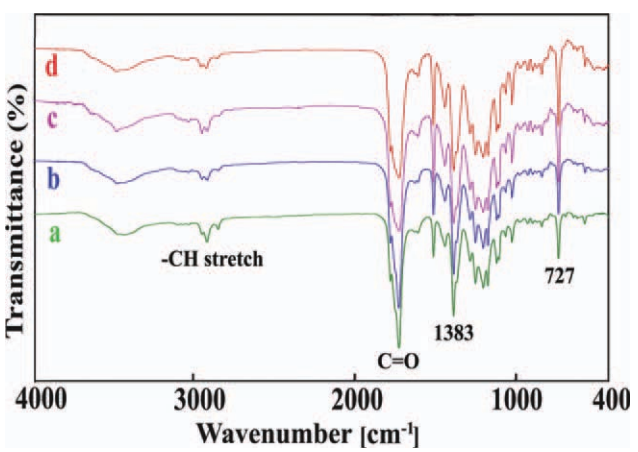

Figure 2 FTIR spectra of (a) PEI, (b) PEI/ZnO BNC (4 wt %), (c) PEI/ZnO BNC (8 wt %), and (d) PEI/ZnO BNC (12 wt %). [Color figure can be viewed in the online issue, which is available at wileyonlinelibrary.com.]

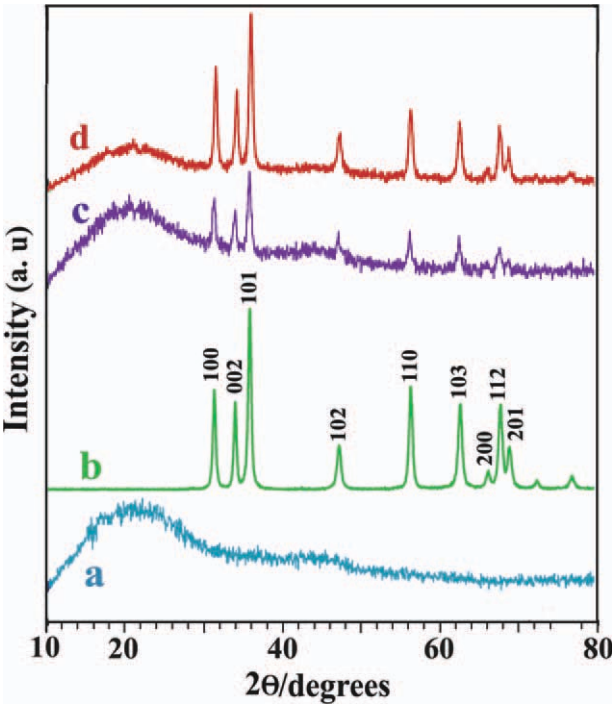

Figure 3 XRD curves of (a) PEI, (b) pure ZnO-NPs, (c) PEI/ZnO BNC (4 wt %), and (d) PEI/ZnO BNC (12 wt %). [Color figure can be viewed in the online issue, which is available at wileyonlinelibrary.com.]

increases with increasing ZnO content. The average crystallite size D was calculated by the Debye–Scherrer formula $D = K\lambda/\beta\cos\theta$, where K is the Scherrer constant, λ the X-ray wavelength, β the peak width at half-maximum, and θ is the Bragg diffraction angle. From the Debye–Scherrer formula, the average crystallite diameter is approximately determined to be 15–22 nm.

Morphology observation

Representative TEM images of PEI/ZnO BNC (12 wt %) are shown in Figure 4. KH550 was used to modify the surface of ZnO-NPs. Hence, the surface energy decreases and the aggregation among particles decreases as well. During the photographing, it can be found that there is no aggregation of a large quantity of particles. Most of the particles are distributed individually as shown in the TEM micrographs. These images confirmed the homogeneous dispersion of modified ZnO-NPs (with the average particle size below 50 nm) in the PEI matrix and representing that the KH550 coupling agent and ultrasonic route play important roles in dispersing the NPs. In comparison with nanocomposite containing functionalized ZnO-NPs by γ-methacryloxypropyltrimethoxysilane (KH570) as a silane coupling agent,

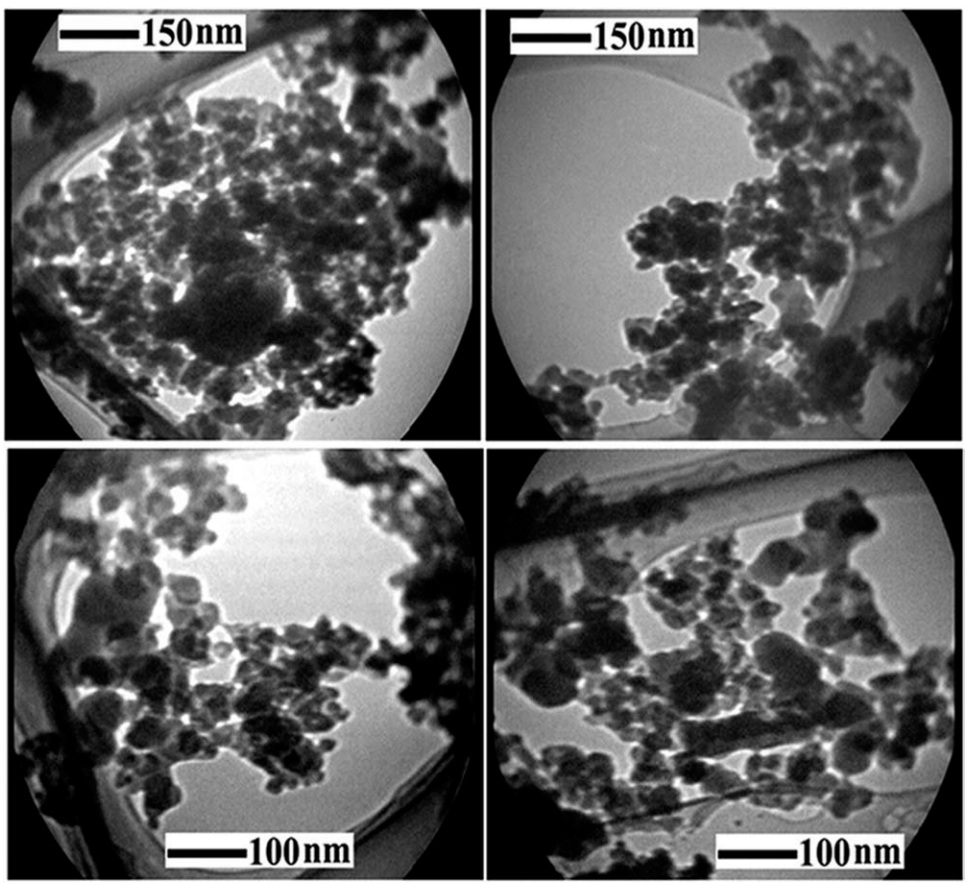

Figure 4 TEM micrographs of PEI/ZnO BNC (12 wt %).

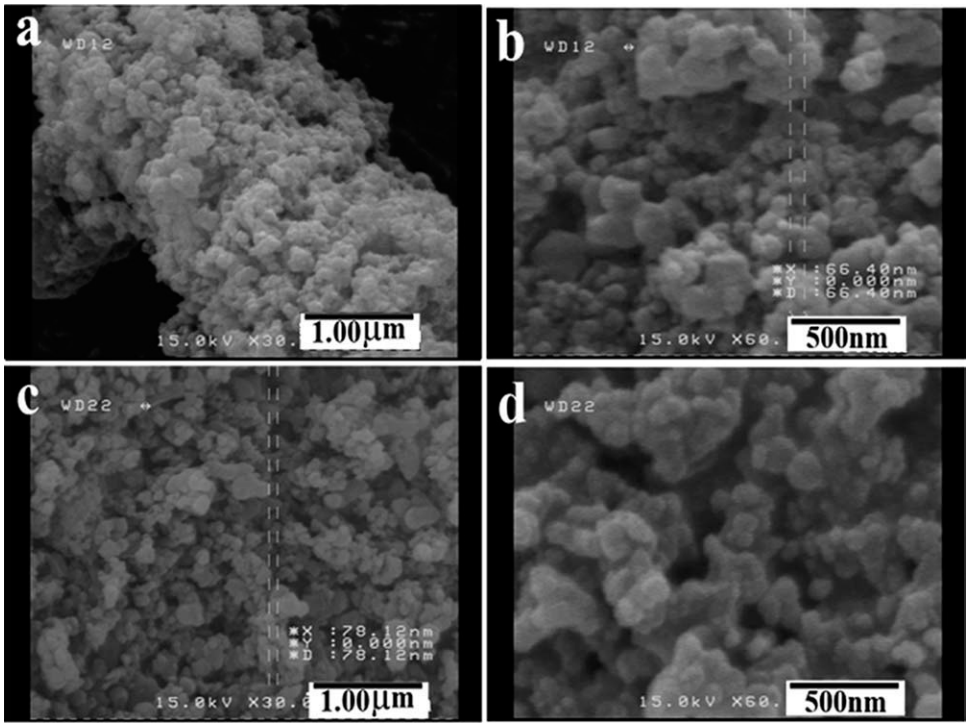

Figure 5 FE-SEM micrographs of (a) PEI, (b,c) PEI/ZnO BNC (8 wt %), and (d,e) PEI/ZnO BNC (12 wt %).

the TEM micrographs of obtained BNCs showed that NPs were uniformly dispersed in the PEI matrix. It has been recognized that the organic nature of coupling agent as a surface modifier is a key factor to promote the dispersion of the NPs in the polymer matrix.[48]

Also, Figure 5 shows the morphology as obtained by FE-SEM micrographs of (a) PEI, (b,c) PEI/ZnO BNC (8 wt %), and (d,e) PEI/ZnO (12 wt %) which demonstrated a homogeneous nanostructure and confirmed that the surface of PEI/ZnO BNCs is in nanoscale compared to the PEI.

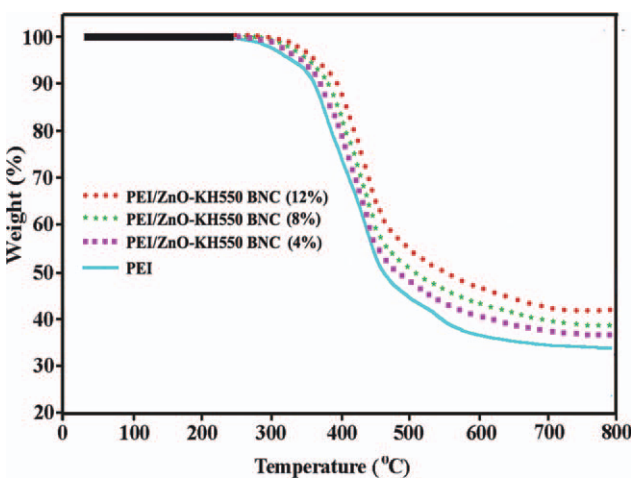

Figure 6 TGA thermograms of PEI and PEI/ZnO BNCs under a nitrogen atmosphere at a heating rate of 10°C/min. [Color figure can be viewed in the online issue, which is available at wileyonlinelibrary.com.]

Thermal properties

The thermal properties of the PEI and PEI/ZnO BNCs were evaluated by means of TGA in a nitrogen atmosphere at a heating rate of 10°C/min. Thermal stabilities were studied based on 5 and 10% weight loss (T_5, T_{10}) of the polymers and residue at 800°C (char yield). TGA data revealed that PEI is thermally stable up to 320°C (Fig. 6). The thermal analysis data of this polymer and obtained BNCs are summarized in Table I. Limiting oxygen index (LOI) values were calculated based on Van Krevelen and Hoftyzer equation.[49]

TABLE I
Thermal Properties of the PEI and PEI/ZnO BNCs

Samples	T_5 (°C)[a]	T_{10} (°C)[b]	Char yield (%)[c]	LOI[d]
PEI	328	360	34	31.1
PEI/ZnO BNC (4 wt %)	343	370	37	32.3
PEI/ ZnO BNC (8 wt %)	353	381	39	33.1
PEI/ ZnO BNC (12 wt %)	360	394	44	35.1

[a] Temperature at which 5% weight loss was recorded by TGA at a heating rate of 10°C/min under a nitrogen atmosphere.
[b] Temperature at which 10% weight loss was recorded by TGA at a heating rate of 10°C/min under a nitrogen atmosphere.
[c] Weight percentage of material left undecomposed after TGA analysis at a temperature of 800°C under a nitrogen atmosphere.
[d] LOI evaluating char yield at 800°C.

$$\mathrm{LOI} = 17.5 + 0.4\,\mathrm{CR}$$

Here, CR represents char yield. From the results obtained, ZnO particles show some stabilizing interaction according to the temperature region and delay the occurrence of cracking in the weight loss stage. Thermal behavior of the BNCs was determined as a function of nano-ZnO content up to 12 wt %. Increasing in the thermal stability may be inconvenient with the high thermal stability of ZnO network and the physical crosslink points of the ZnO particles, which restricted the motion of the molecular chain of PEI. The char yield of pure PEI at 800°C is 34%, whereas those of the bionanocomposites (PEI/ZnO BNC: 4, 8, and 12 wt %) at 800°C is in the range of 37–44%. On the basis of LOI values (32–35), all macromolecules can be classified as the self-extinguishing BNC polymers.

CONCLUSIONS

Based on the analysis of the results of the experimental study, the following conclusions can be arrived: An amino acid-based PEI with chiral main chain was successfully synthesized. This polymer was prepared via direct polyesterification of *N*,*N*′-(pyromellitoyl)-bis-(L-tyrosine dimethyl ester) as a biodegradable optically active diphenolic monomer and synthesized diacid containing L-methionine. The amorphous morphology and incorporation of L-tyrosine with ester linkage into PEI backbone gave polymer with remarkable solubility in common organic solvents. The synthesized polymer having both optically active and thermally stable properties is required for the column chromatography at high temperature for the separation of enantiomeric mixtures. After that, PEI/ZnO BNCs were prepared using the nano-ZnO surface coupled by KH550 via sonochemical reaction which can accelerate hydrolysis, increase collision chance for the reactive system, and improve the dispersion of the NPs in the polymer matrix. The FE-SEM and TEM outcomes indicated that the NPs were dispersed homogeneously in PEI matrix on nanoscales. TGA confirmed that the heat stability of the BNC polymers was enhanced in the existence of modified nanostructure ZnO particles.

The authors express their gratitude to the Research Affairs Division Isfahan University of Technology (IUT), Isfahan, for partial financial support.

References

1. Chivrac, F.; Pollet, E.; Averous, L. Mat Sci Eng R 2009, 67, 1.
2. Kumar, P.; Sandeep, K. P.; Alavi, S.; Truong, V. D.; Gorga, R. E. J Food Eng 2010, 100, 480.
3. Gilman, J. W. Appl Clay Sci 1999, 15, 31.
4. Gilman, J. W.; Jackson, C. L.; Morgan, A. B.; Harris, R. Jr.; Manias, E.; Giannelis, E. P.; Wuthenow, M.; Hilton, D.; Phillips, S. H. Chem Mater 2000, 12, 1866.
5. Porter, D.; Metcalfe, E.; Thomas, M. J. K. Fire Mater 2000, 24, 45.
6. Armes, S. P. Polym News 1995, 20, 233.
7. Huynh, W. U.; Peng, X.; Alivisatos, A. P. Adv Mater 1999, 11, 923.
8. Godovski, D. Y. Adv Polym Sci 1995, 119, 79.
9. Okada, A.; Usuki, A. Mater Sci Eng C 1995, 3, 109.
10. Yokoyama, R.; Suzuki, S.; Shirai, K.; Yamauchi, T.; Tsubokawa, N.; Tsuchimochi, M. Eur Polym J 2006, 42, 3221.
11. Rajh, T.; Tiede, D. M.; Thurnauer, M. C. J Non-Cryst Solids 1996, 207, 815.
12. Dang, Z. M.; Fan, L. Z.; Zhao, S. J.; Nan, C. W. Mater Res Bull 2003, 38, 499.
13. Ringwald, S. C.; Pemberton, J. E. Environ Sci Technol 2000, 34, 259.
14. Agrawal, M.; Gupta, S.; Zafeiropoulos, N. E.; Oertel, U.; Habler, R.; Stamm, M. Macromol Chem Phys 2010, 211, 1925.
15. Bourgeat-Lami, E.; Espiard, Ph.; Guyot, A. Polymer 1995, 36, 4385.
16. Ratna, D.; Divekar, S.; Samui, A. B.; Chakraborty, B. C.; Banthia, A. K. Polymer 2006, 47, 4068.
17. Siengchin, S.; Karger-Kocsis, J.; Apostolov, A. A.; Thomann, R. J Appl Polym Sci 2007, 106, 248.
18. Wang, Q.; Xia, H.; Zhang, C. J Appl Polym Sci 2001, 80, 1478.
19. Xu, X.; Li, B.; Lu, H.; Zhang, Z.; Wang, H. Appl Surf Sci 2007, 254, 1456.
20. Sawai, J. J Microbiol Methods 2003, 54, 177.
21. Kamat, P. V.; Huehn, R.; Nicolaescu, R. J Phys Chem B 2002, 106, 788.
22. Wu, J.; Xie, C. S.; Bai, Z. K.; Zhu, B. L.; Huang, K. J.; Wu, R. Mater Sci Eng B 2002, 95, 157.
23. Wu, R.; Xie, C. S. Mater Res Bull 2004, 39, 637.
24. Kitano, M.; Shiojiri, M. Powder Technol 1997, 93, 267.
25. Kumar, S. A.; Chen, S. M. Anal Lett 2008, 41, 141.
26. Wang, J. X.; Sun, X. W.; Wei, A.; Lei, Y.; Cai, X. P.; Li, C. M.; Dong, Z. L. Appl Phys Lett 2006, 88, 233106.
27. Tang, E.; Cheng, G.; Pang, X.; Ma, X.; Xing, F. Colloid Polym Sci 2006, 284, 422.
28. Adrova, N. A.; Artyukhov, A. I.; Baclagina, Y. U. G.; Borisova, T. I.; Koton, M. M.; Mikhailova, N. V.; Nikitin, V. N.; Sidorovich, A. V. Vysokomol soyed 1973, A15, 153.
29. Li, C. H.; Chen, C. C.; Chen, K. M. J Appl Polym Sci 1994, 52, 1751.
30. Hsu, T. F.; Lin, Y. C.; Lee, Y. D. J Polym Sci Polym Chem 1998, 36, 1791.
31. Iannelli, M.; Alupei, V.; Ritter, H. Tetrahedron 2005, 61, 1509.
32. Mallakpour, S.; Zadehnazari, A. Express Polym Lett 2011, 5, 142.
33. Mallakpour, S.; Kolahdoozan, M. J Appl Polym Sci 2007, 104, 1248.
34. Mallakpour, S.; Tirgir, F.; Sabzalian, M. R. J Polym Res 2011, 18, 373.
35. Mallakpour, S.; Zeraatpisheh, F. Colloid Polym Sci 2011, 289, 1055.
36. Higashi, F.; Ong, C. H.; Okada, Y. J Polym Sci A Polym Chem 1999, 37, 3625.
37. Higashi, F.; Akiyama, N.; Takahashi, I.; Koyama, T. Polym Sci Polym Chem Ed 1984, 22, 1653.
38. Mallakpour, S. E.; Hajipour, A. R.; Habibi, S. J Appl Polym Sci 2002, 86, 2211.
39. Mallakpour, S.; Habibi, S. Eur Polym J 2003, 39, 1823.

40. Mallakpour, S.; Tirgir, F.; Sabzalian, M. R. Amino Acids 2011, 40, 611.
41. Mallakpour, S.; Zeraatpisheh, F.; Sabzalian, M. R. J Polym Environ 2011, DOI: 10.1007/s10924–011-0308–2.
42. Shenhar, R.; Norsten, T. B.; Rotillo, V. M. Adv Mater 2005, 17, 657.
43. Yao, Q.; Zhou, Y.; Sun, Y.; Ye, X. J Inorg Organomet Polym 2008, 18, 477.
44. Gu, F.; Wang, S. F.; Lu, M. K.; Zhou, G. J.; Xu, G.; Yuan, D. R. Langmuir 2004, 20, 3528.
45. Ogasawara, T.; Nara, A.; Okabayashi, H.; Nishio, E.; O'Connor, C. J. Colloid Polym Sci 2000, 278, 946.
46. Compton, O. C.; Mullet, C. H.; Chiang, S.; Osterloh, F. E. J Phys Chem C 2008, 112, 6202.
47. Li, S. J Biomed Mater Res (Appl Biomater) 1999, 48, 342.
48. Mallakpour, S.; Zeraatpisheh, F. Des Monomers Polym 2011, 14, 487.
49. Van Krevelen, D. W.; Hoftyzer, P. J. Properties of Polymers, 3rd ed.; Elsevier: Amsterdam, 1976.